B cell tolerance checkpoint function in multiple sclerosis and transient CD52 depletion

Anastasia Alexaki[1], Fotis Baltoumas[2], Dimitrios Tzanetakos[3], Chrysoula Zografou[4], Galini Kyriakaki[1], Aglaia G. Vakrakou[1], Maria Anagnostouli[1], Georgia Karadima[1], Marinos C. Dalakas[1,5], Leonidas Stefanis[1], Konstantinos Kilidireas[1], Kevin C. O'Connor[6], Georgios Pavlopoulos[2], Panos Stathopoulos[1*].

1. First Department of Neurology, National and Kapodistrian University of Athens, Greece.

2. Institute for Fundamental Biomedical Research, Biomedical Science Research Center 'Alexander Fleming', Vari, Greece.

3. Second Department of Neurology, National and Kapodistrian University of Athens, Greece.

4. MABY, Monoclonal Antibody Discovery, Biomedical Science Research Center 'Alexander Fleming', Vari, Greece.

5. Neuroimmunology Unit, Department of Pathophysiology, Faculty of Medicine, National and Kapodistrian University of Athens, Greece.

6. Departments of Neurology and Immunobiology, Yale School of Medicine, New Haven, CT, USA.

*Corresponding author: Panos Stathopoulos, First Department of Neurology, Papadiamantopoulou 21, 11518 Athens, Greece. Email: pmstathopoulos@gmail.com; panosst@eginitio.uoa.gr.

Word count 4963

Abstract

The anti-CD52 monoclonal antibody (mAb) alemtuzumab is highly effective in treating relapsing-remitting multiple sclerosis (RRMS) but often leads to secondary autoimmunity. Understanding its impact on B cell tolerance mechanisms is crucial for deciphering both B cell involvement in RRMS and development of secondary autoimmunity. Previous investigations indicate that between the two B cell tolerance checkpoints, only the peripheral checkpoint is dysfunctional in RRMS.

To evaluate peripheral B cell tolerance checkpoint integrity in alemtuzumab-treated RRMS patients and healthy/disease controls, we used an established approach and constructed 128 recombinant mAbs from single IgM+CD27-CD19+CD10- mature naïve B cells; these were subsequently tested their poly- and autoreactivity by ELISA. We examined mAbs from three healthy donors (HDs), three immunotherapy-naïve MS patients, and six patients treated with alemtuzumab at comparable time points post-treatment (mean ± SD 3.7 ± 0.67 years); of those, three had developed secondary autoimmunity. In parallel, we investigated B cell receptor repertoire parameters associated with tolerance mechanisms in the same subject groups.

Polyreactivity of mature naïve B cell-derived mAbs did not differ among subject groups. In mAb autoreactivity measurements that define peripheral checkpoint integrity, we observed that two of three immunotherapy-naïve RRMS patients had a defective peripheral checkpoint. Among patients treated with alemtuzumab, a bimodal distribution was noted: three of six patients had a high fraction of autoreactive mAbs, pointing to a defective peripheral checkpoint, and three had an autoreactive fraction significantly lower than that of HDs (P=0.027). This bimodal distribution did not align with presence of secondary autoimmunity. Further, alemtuzumab-treated patients showed lower mean naïve B cell complentarity-determining region 3 (CDR3)

net charge than HDs (P=0.036). No differences were found in naïve B cell IGKJ1 usage frequency (a measure of the extent of secondary VJ recombination) among the three subject groups. Examination of memory CDR3 properties revealed differences between alemtuzumab-treated patients and controls in the IgD compartment.

In conclusion, our most remarkable finding was that in a subset of alemtuzumab-treated patients the fraction of autoreactive mature naive B cells, defining peripheral tolerance checkpoint function, was extraordinarily low compared to healthy and disease controls in this study as well as previous reports. This phenomenon could be connected to the improvement of the function of T regulatory cells, known to be defective in MS and to influence peripheral checkpoint function, as well as to a deep depletion of B cells up to the pre-B cell stage.

Key words: Multiple sclerosis; alemtuzumab; B cell tolerance; secondary autoimmunity.

Abbreviations: AIRE, Autoimmune Regulator; BCR, B Cell Receptor; CBA, Cell-Based Assay; CDR3, Complementarity-Determining Region 3, GFP, Green Fluorescent Protein; HDs, Healthy Donors; Hep-2, Human Epithelial Cells Type 2; IgH, Immunoglobulin Heavy Chain; IgK, Immunoglobulin Kappa Light Chain; IgL, Immunoglobulin Lambda Light Chain, IRTs, Immune Reconstitution Therapies; MS, Multiple Sclerosis; mAb, Monoclonal Antibody; NGS, Next-Generation Sequencing; PBMCs, Peripheral Blood Mononuclear Cells; RRMS, Relapsing-Remitting Multiple Sclerosis; SHMs, Somatic Hypermutations; SLE, Systemic Lupus Erythematosus;

T1D, Type 1 Diabetes; Tregs, Regulatory T Cells; TSHR, Thyroid-Stimulating Hormone Receptor

Introduction

Multiple sclerosis (MS) is the most common autoimmune disease of the central nervous system and the leading cause of non-traumatic neurological disability in young adults[1–3]. It is associated with genetic and non-genetic risk factors[4,5], and is immunopathologically[6–8] characterized by demyelination, acute and chronic inflammation, axonal and neuronal degeneration. From a clinical standpoint, MS has been historically classified into subtypes, the more common being relapsing-remitting MS (RRMS)[9], with partial or nearly complete recovery of symptoms between attacks.

Even though T cell contributions have been extensively studied in both humans and animal models[10,11], the high clinical efficacy of anti-CD20 therapies has highlighted the crucial role of B cells in disease pathogenesis[12]. Physiologically, as B cells mature in the bone marrow, V(D)J gene recombination generates the necessary B cell receptor (BCR) diversity to shield against infection and at the same time autoreactive BCRs. These autoreactive B cells are removed by two tolerance checkpoints. The first, central tolerance checkpoint is found between the pre-B to immature B cell transition and the second, peripheral checkpoint, between the new emigrant to mature naive B cell transition. Defects in central and peripheral tolerance checkpoint function have been found in almost all autoimmune diseases that have been examined[13–15]. In RRMS, a defective central (in 2 out of 7 patients) and mainly a defective peripheral tolerance checkpoint (in 7 out of 7 patients) have been demonstrated[16].

A critical question is whether the demonstrated defects in tolerance checkpoint function can be reversed with targeted immunotherapy. In type 1 diabetes (T1D), treatment with the anti-CD20 monoclonal antibody (mAb) could not restore the

damaged integrity of the peripheral checkpoint[17]. In contrast to continuous immunotherapy regimens, most of which result in chronic and sometimes increasing immunosuppression, immune reconstitution therapies (IRTs)[18] (alemtuzumab, cladribine, autologous hemopoietic stem cell transplantation) are administered once or twice and promote immune system renewal and drug-free disease remission. The mAb alemtuzumab targets CD52+ immune cells (T and B cells, monocytes, natural killer (NK) cells, eosinophils and dendritic cells) causing their temporary depletion and renewal within weeks, months, or years, depending on the cell type. Clinically, alemtuzumab is very effective in diminishing MS disease activity[19], however its application is limited by frequent development of secondary autoimmune phenomena, most commonly thyroid-related[19,20].

CD52+ B cell depletion differs from CD20+ B cell depletion. First, CD52, but not CD20, is expressed on pre-B cells[21], and accordingly anti-CD52 therapy affects a deeper depletion of B cells. Second, CD52—but not CD20 depletion—is followed by the generation of a high frequency of naïve B cells that exceeds baseline levels[22,23]. With all that in mind and in order to better understand efficacy and side effects of alemtuzumab, as well as B cell implication in RRMS and secondary autoimmunity, we evaluated the impact of alemtuzumab on B cell tolerance mechanisms. We first assessed the peripheral B cell tolerance checkpoint integrity with a historical, established and validated method involving cloning of individual mature naïve B cells and examination of their poly- and autoreactivity. Next, we inquired whether next-generation sequencing (NGS)[24] of the BCR can identify alterations in tolerance mechanisms present in either immunotherapy-naïve RRMS patients or in patients

treated with alemtuzumab. Finally, we examined if tolerance parameters correlate with clinical outcomes.

Materials and Methods

Patients, specimens, and study approval

Peripheral blood was collected from healthy donors (HDs) and RRMS patients (immunotherapy-naïve or treated with alemtuzumab) after obtaining informed consent. Patients were diagnosed[25], treated with alemtuzumab (12 mg/day iv for 5 consecutive days, followed one year later by 12 mg/day for 3 days), and followed at Eginitio University Hospital. For alemtuzumab-treated patients, samples were collected at least one year after the second treatment cycle; patients were categorized based on subsequent 1. MS activity (clinical and radiological) and 2. presence of secondary autoimmune manifestations. The three groups (HDs, immunotherapy-naïve RRMS and alemtuzumab-treated patients) were matched for age and sex. Peripheral blood mononuclear cells (PBMCs) were separated using Ficoll (PAN-Biotech) gradient fractionation and cryopreserved in liquid nitrogen vapors. The study was approved by the Institutional Review Board of Eginitio Hospital. Two of the three healthy donor specimens (HD01 and HD02), were processed previously in the Laboratory of Dr. O'Connor at Yale University[15].

PTPN22 R620W/C1858T variant genotyping

A previously described[26] protocol was applied. Briefly, DNA extraction from whole blood (QIAamp DNA Blood Mini Kit, Qiagen) was followed by PCR amplification of the R620W/C1858T variant-containing PTPN22 region (Taq DNA Polymerase and dNTPs, Thermo Fisher Scientific; primers, Integrated DNA Technologies) and Sanger sequencing.

B cell isolation, staining and single-cell sorting

A previously established[14,15,26,27] protocol was followed. Briefly, cryopreserved PBMCs were thawed, and B cells were positively selected using a biotin antibody cocktail with magnetic streptavidin nanobeads (MojoSort human pan B cell isolation kit, BioLegend). The isolated B cells were then stained with anti-human CD10 antibody-PE/cyanine7, CD19-pacific blue, CD27-PerCP/cyanine5.5 (BioLegend), IgM-FITC, CD21-APC, and IgG-PE (BD Biosciences). Single mature naïve B cells (IgM^+, IgG^-, $CD21^+$, $CD27^-$, $CD19^+$, $CD10^-$) were sorted into 96-well plates using a FACSAria flow cytometer (BD) and immediately frozen on dry ice and stored at -80°C until further use.

mAb production

An established[14] approach was used for mAb production. For each B cell, matching heavy (IgH) and light (IgK and IgL) chain variable immunoglobulin regions were amplified by a nested PCR from cDNA, cloned into expression vectors, and sequenced. The sequences were analyzed with IgBlast (http://www.ncbi.nlm.nih.gov/projects/igblast) and IMGT/V-QUEST (http://www.imgt.org)[28,29]. HEK 293A cells were then co-transfected with the heavy and light chain vectors, the supernatant was harvested and either used for IgG and polyreactivity ELISAs or purified with the use of protein G beads, quantified and used for autoreactivity ELISAs and the thyroid stimulating hormone receptor (TSHR) live cell-based assay (CBA). Each mAb was cloned, expressed and tested in duplicate.

ELISA

Established[14,15,26] protocols were followed for ELISAs. Briefly, mAb concentrations were measured in HEK supernatants with a sandwich ELISA using anti-human IgG antibodies (Jackson Laboratories). Supernatants were then tested for polyreactivity, defined as reactivity against three different antigens: dsDNA, LPS, and insulin (all by Sigma-Aldrich)[26]. Autoreactivity was determined by application of purified mAbs to microplates precoated with human epithelial cell lysate (QUANTA Lite, INOVA Diagnostics).

Live CBA for the detection of Thyroid-Stimulating Hormone Receptor (TSHR) antibodies

mAbs were assessed for TSHR binding with a previously described flow cytometric live CBA[14,30,31]. In brief, HEK 293T cells were transfected with a plasmid vector encoding human TSHR-GFP (TSHR -Green Fluorescent Protein; kind gift from MABY and Dr. Bieberman of Charite University Hospital). After forty-eight hours, the transfected cells were incubated with 2 µg/mL of mAb, and subsequently with a secondary, Alexa fluor 647-labeled anti-human IgG antibody (1:1000, Jackson Laboratories). Fluorescence was measured with a BD FACS Canto cytometer. Positivity was assessed by calculating the delta mean fluorescence intensity (ΔMFI) index (percentage of Alexa fluor 647 MFI of TSRH-GFP-transfected cells minus that of non-transfected cells) with FlowJo v10 (BD). The commercial anti-human TSHR mAb clone m22 (ABCDY antibodies, kind gift from MABY) served as a positive control. The cutoff for positivity was applied at the control mean + 4SDs.

cDNA libraries construction and BCR sequencing

RNA was isolated from PBMCs with the QIAwave RNA Mini Kit (Qiagen). cDNA libraries were prepared with the New England Biolabs Next® Immune Sequencing Kit (Human, New England Biolabs), according to the manufacturer's instructions and our previous studies[24,32]. Briefly, reverse transcription employed biotin-labeled primers and addition of a unique molecular identifier (UMI). cDNA was purified using streptavidin magnetic beads, and IgH and IgK/IgL or just IgH variable regions were amplified by a series of two PCRs and quantified with a Bioanalyzer (Agilent). DNA libraries were pooled equimolarly, followed by high throughput 2x300bp paired-end sequencing with a 20% PhiX spike, except for performing 325 cycles for read 1 and 275 cycles for read 2, on either the Illumina MiSeq or NextSeq.

Raw data quality control

Quality control was performed using a slightly modified pRESTO workflow[24,33]. First, reads with a mean Phred quality score >20 and without a valid C-region primer (maximum error rate: primer 0.2, template-switch 0.5) were discarded. Both template-switch additions and C-region primer sequences were deleted from the reads. Both IgH and IgK/IgL primers were used to improve sampling and increase the number of analyzed reads. Reads with identical UMIs were categorized into a single consensus sequence for each UMI, while UMI reads with error scores >0.1 or majority isotypes frequency < 0.6 were removed. If multiple isotypes were identified within a single UMI read group, the consensus sequence was generated using only the reads assigned to the majority isotype. UMI consensus sequence mate-pairs were initially assembled de novo into full-length Ig sequences, requiring a minimum overlap length of 8 bp, a maximum error rate of 0.3, and a p-value threshold of $1 \times 10^{\square\square}$. Mate-pairs that could not be assembled de novo (e.g. due to long CDR3 sequences preventing

overlap) were instead aligned to the 202248-3 release (November 30, 2022) of the International Immunogenetics Information System (IMGT) V-segment germlines, with a minimum identity threshold of 0.5 and an E-value cutoff of $1 \times 10^{-}$. A secondary isotype assignment was performed by aligning the tail (J segment end) of the UMI consensus sequences to a set of sequences anticipated to be upstream of the C region primer. These reference sequences were derived from the IMGT C region and J segment consensus database. Following preprocessing, V(D)J germline segments were assigned, using the IgBLAST search algorithm[28]

BCR repertoire analysis

Reported germline sequences, combined with the C-region annotation, were used to define the locus and isotype. IgBLAST results were parsed and standardized using ChangeO,[24] and filtered to include only productive BCR sequences. Genotyping was performed using TIgGER.[24] Germline sequences of each assigned clonal group were identified using Change-O. The genotyped, clonal-assigned reads were used to calculate somatic hypermutations (SHMs) with SHazaM, by comparing observed sequences against the germline. With the SHM frequencies calculated, a 1% (of nucleotides) mutational cutoff was set to separate naive and memory BCRs (for both IgH and IgK/IgL). V- and J-gene (IgH and IgK/IgL) family usage was calculated as the percentage of unique sequences assigned to a given gene family within the total number of sequences for each isotype in each compartment (naïve/memory). Variations in the usage of IgK V-gene sequences were evaluated by calculating the proportion of upstream (distal) vs. downstream (proximal) V-gene families. The definition of IgK V-gene sequences as upstream or downstream was based on annotations provided by IMGT. IgH CDR3 properties[24,34] (amino acid sequence

length, hydrophobicity -estimated as the grand average hydropathy index, or GRAVY-, net charge, polarity, acid chain bulkiness, aliphatic index, as well as the ratios of aromatic, acidic, and basic amino acid residues) were measured separately for naive and memory sequences using Alakazam[24].

Statistical analysis

Data were plotted and analyzed with the GraphPad Prism software version 8.3.1. Unpaired t-tests and one-way ANOVA tests were performed to compare means between different groups. P-values below 0.05 (two-tailed) were considered statistically significant.

Results

Study subjects and production of mAbs

Study subjects included five healthy donors, four immunotherapy-naive RRMS patients, and nine alemtuzumab-treated RRMS patients (**Table**). Age and sex distribution did not differ significantly between the three patient groups. Alemtuzumab-treated patients were sampled 2.2 to 4.8 years [mean ± standard deviation (SD) 3.7 ± 0.67 years] post treatment initiation, so length of follow-up and degree of immune reconstitution at the time of sampling were comparable between treated patients. Six of the alemtuzumab-treated patients had suffered secondary autoimmune complications, including Graves' disease (two patients), Hashimoto thyroiditis (two patients), and immune thrombocytopenic purpura (two patients, **Table**). To assess B cell tolerance mechanisms, we produced 127 mAbs—in biological duplicates—from single mature naïve B cells (IgM^+, IgG^-, $CD21^+$, $CD27^-$, $CD19^+$, $CD10^-$) of 12 subjects. Sequences of the cloned variable regions were compared to the germline using IMGT/V-QUEST and IgBLAST, and mutated sequences were excluded from the analysis as previously described[14] (**Supplementary Table 1**). Importantly, carriers of the C1858T PTPN22 polymorphism, associated with defective central and peripheral B cell tolerance checkpoint function[16], were excluded from all subject groups.

Polyreactivity of mature naïve B cells is similar in HDs, RRMS patients, and alemtuzumab-treated RRMS patients

To determine whether anti-CD52 treatment with alemtuzumab affects the frequency of polyreactive mature naïve B cells, we used an established and extensively validated experimental approach that tests reactivity of mature naïve B cell-derived mAbs against three antigens: dsDNA, LPS, and insulin, with polyreactivity being defined as reactivity against all three antigens. The fraction of polyreactive mAbs ranged from 9% to 14.29% in HDs (mean ± SD 10.57 ± 3.24 %), from 7.29% to 12.50% in immunotherapy-naïve RRMS patients (10.9 ± 2.7%), and from 8.33% to 14.29% in patients with RRMS treated with alemtuzumab (11.5 ± 2.3%) (**Fig. 1**). Polyreactive mAb percentages did not differ significantly between the three groups. Furthermore, the fraction of polyreactive mAbs did not differ significantly between alemtuzumab treated patients that developed secondary autoimmunity (Ale03, Ale33, Ale25) and those that did not (Ale27, Ale40, Ale46).

A subset of alemtuzumab-treated patients exhibit a very low fraction of autoreactive mature naïve B cells

The peripheral B cell tolerance checkpoint integrity was assessed by examining purified, mature naïve B cell-derived mAbs for potential autoreactivity, i.e. reactivity against human epithelial type two (HEp-2) cell lysate[16] (**Fig. 2**). After performing HEp-2 ELISA, we found that the percentage of autoreactive mAbs ranged from 19.05 to 33.33% in HDs (mean ± SD 26.55 ± 7.17%), and from 23.08 to 37.50% (32.7 ± 8.33%) in immunotherapy-naïve RRMS patients. This difference did not reach statistical significance, likely due to the small sample size and variance in HDs (P = 0.3). Despite that and as peripheral checkpoint dysfunction is characterized by an

autoreactive fraction of (at least) around 40%[13], we suggest that the function of the peripheral checkpoint may be compromised in two out of three RRMS patients.

In patients treated with alemtuzumab, we observed a more contrasting bimodal distribution. In three of six patients, the percentage of autoreactive mAbs was high (36.36% in Ale40 and 37.50% in Ale03 and Ale33 37.50% (mean ± SD 37.12 ± 0.66%), pointing to defective peripheral B cell tolerance function (**Fig. 2**). This defective function could be attributed to the disease itself, the effect of CD52 cell depletion, or a combination of both. In the remaining three alemtuzumab-treated RRMS patients, we observed an extraordinarily low autoreactive fraction, with percentages ranging from 8.33 to 14.29% (14.29% in Ale27, 11.11% in Ale46, and 8.33% in Ale25 (mean ± SD 11.24 ± 3%). Autoreactive fractions in this subset of patients were lower than those of HDs (26.55 ± 7.17%; P for the post-hoc comparison = 0.027) as well as those of immunotherapy-naïve RRMS patients (32.7 ± 8.33%, P for the post-hoc comparison = 0.0137). In addition, such frequencies have never been observed in HDs or RRMS patients previously[13]. Therefore, this effect is most likely explained by the preceding CD52+ cell depletion. Of the three patients with a low autoreactive mature naïve mAb/BCR fraction, one had manifested secondary autoimmunity in the form of Graves' disease (**Table**); thus, a low autoreactive fraction does not preclude secondary autoimmunity. Moreover, there was no significant difference in time between alemtuzumab dosing and sample acquisition between alemtuzumab-treated patients with a high and a low mature naïve B cell autoreactive fraction (**Table**).

Mature naïve-derived mAbs from RRMS patients treated with alemtuzumab do not bind Graves' disease autoantigen TSHR

Almost 50% of alemtuzumab-treated RRMS patients develop secondary, thyroid-related autoimmunity, commonly Graves' disease[19,20], a condition associated with autoantibodies against the TSHR[35]. With that in mind, we asked whether mature naïve B cell-derived mAbs from two RRMS patients treated with alemtuzumab that developed TSHR autoantibody-positive Graves' disease bound TSHR. Of note, only one of these two patients had a compromised peripheral B cell tolerance checkpoint. mAbs produced from mature naïve B cells of HDs, immunotherapy-naïve RRMS patients and alemtuzumab-treated patients that did not develop Graves' disease served as negative controls. A commercial mAb against the TSHR was used as a positive control[36] (**Supplementary Fig. 1**). None of the 95 mAb tested bound the TSHR (**Supplementary Table 2**), indicating that even in the one patient with defective peripheral tolerance B cell function and Graves' disease, autoimmunity likely initiates beyond the lymphnode/T cell help stage of B cell development and not in the naïve stage prior to the encounter of the (auto)antigen.

Few naïve B cell IgH CDR3 properties differ between HDs and RRMS patients

As the established approach to assess B cell tolerance is time-consuming and laborious, we sought to investigate whether BCR NGS could evaluate B cell tolerance checkpoint integrity to a similar extent or perhaps with enhanced sensitivity. To that end, we performed BCR NGS out of total PBMC RNA for the indicated HD, immunotherapy-naïve RRMS and alemtuzumab-treated RRMS samples (**Table**). After raw data quality control, we applied a 1% mutational cutoff to separate naïve from memory IgH sequences, yielding percentages comparable[37] to immunophenotypic

profiling of HDs (**Supplementary Table 3**). With that separation, we were able to reproduce known differences in CDR3 properties between memory and naïve B cells [34] (**Supplementary Fig. 2**).

Several reports[26,34,38–40] have indicated that IgH CDR properties might be a measure for autoreactivity and compromised B cell tolerance; therefore we examined whether these differ between in the naïve compartment of HDs, immunotherapy-naïve RRMS patients and RRMS patients treated with alemtuzumab (**Fig. 3**). As IgA, IgE, and IgG counts were unsurprisingly limited in the naïve pool, they were excluded from the analysis. Of all nine CDR3 properties examined, only two were found to differ significantly between subgroups. First, net charge was found to be lower in alemtuzumab-treated RRMS patients compared to HDs (IgD+IgM+ mean ± SD -0.49 ± 0.04 vs. -0.38 ± 0.036), and this was evident in the IgD compartment (P = 0.0121), the IgM compartment (P = 0.0066), as well as in their sum (P = 0.0036). The comparison of immunotherapy-naïve RRMS patients to HDs for the sum of IgD and IgM was borderline insignificant (P = 0.0615), possibly due to the lower N. Second, basic abundance was found to be lower in alemtuzumab-treated RRMS patients (0.1 ± 0.01) compared to HDs (0.11 ± 0.01), albeit only in the IgD fraction (P = 0.027). Differences in CDR3 length and polarity did not reach significance, likely due to low N. CDR3 properties did not correlate with clinical outcomes (**Fig. 3**). We also examined if CDR3 properties correlate with peripheral tolerance defects as determined by the autoreactivity ELISA; this however was not the case (**Supplementary Fig. 3**). Overall, analysis of IgH CDR properties revealed subtle differences between HDs and RRMS patients (these differences were significant for comparisons of HDs with alemtuzumab-treated patients likely due to the higher N of

seven in that group, as opposed to the N of four in the immunotherapy-naïve RRMS group) but did not show differences between immunotherapy-naïve and alemtuzumab-treated RRMS patients.

Naïve B cell usage of *Jk1*, downstream *Jk3,4,5*, and upstream *Vk* gene segments does not differ between HDs, immunotherapy-naïve and alemtuzumab-treated RRMS patients

VJ recombination in the Igk locus occurs in two stages: the first (primary), generating diversity and the second, replacing autoreactive BCRs with non-reactive ones in the context of central B cell tolerance mechanisms[41–43]. Increased repertoire frequency of the *Jk1* gene segment has been associated with increased frequency of primary recombination, while increased frequency of the downstream *Jk3,4,5* gene segments, as well as of the upstream *Vk* genes with increased secondary rearrangements[44,45]. Here, *Jk1* frequency was comparable in HDs, immunotherapy-naïve, and alemtuzumab-treated RRMS patients (P for one-way ANOVA = 0.62) (**Fig. 4A**). Similarly, naïve B cell usage of upstream *Vk* and downstream *Jk3,4,5* gene segments did not consistently separate subject groups (**Fig. 4B**). These collective data suggest that secondary recombination is not increased in RRMS (immunotherapy-naïve and alemtuzumab-treated).

Memory B cell CDR3 properties may separate alemtuzumab-treated patients from HDs and untreated RRMS patients

Since analysis of the naïve BCR repertoire and IgH CDR3 properties did not result in profound differences between subject groups, we investigated the memory B cell repertoire in search of immunological characteristics that reflect secondary

autoimmune manifestations affected by CD52+ immune cell depletion. Previous studies[46,47] of auto- and polyreactivity of single B cells from the IgM and the IgG memory compartment of HDs had found that a large fraction of IgM memory B cells display low poly- and autoreactivity (compared to mature naïve B cells) while the frequency is higher in IgG memory B cells. Here, we analyzed the memory compartment CDR3 properties in the three subject groups (HDs, immunotherapy-naïve and alemtuzumab-treated RRMS) per immunoglobulin class (**Fig. 5**). Significant differences were observed only in the IgD compartment. Specifically, alemtuzumab-treated RRMS patients showed a significantly increased CDR3 length (mean ± SD 16.18 ± 0.6) compared to HDs (15.07 ± 0.24; P = 0.012), while the comparison between alemtuzumab-treated and immunotherapy-naïve RRMS patients (15.6 ± 0.6) did not reach significance (P=0.112). Importantly, polarity was significantly decreased in alemtuzumab-treated patients (8.4 ± 0.1) compared to both HDs (8.6 ± 0.06; P = 0.039) and RRMS patients (8.5 ± 0.06; P = 0.045). Finally, aromatic abundance was higher in alemtuzumab-treated patients (0.23 ± 0.02) than in HDs (0.2 ± 0.02, P = 0.021), but did not differ compared to immunotherapy-naive RRMS patients (0.22 ± 0.02; P = 0.510). Of note, in none of these IgD CDR3 properties (length, polarity, and aromatic abundance) did immunotherapy-naive RRMS patients differ significantly from HDs (CDR3 length: P = 0.293; polarity: P = 0.558; aromatic abundance: P = 0.09). CDR3 properties did not correlate with clinical outcomes (**Fig. 5**). Taken together, these differences represent interesting but isolated findings of an exploratory analysis that warrant confirmation in larger studies.

The usage of *Jk1*, downstream *Jk3,4,5*, and upstream *Vk* gene segments in memory B cells is consistent across HDs, RRMS patients, and alemtuzumab-treated RRMS patients.

Similar to the naïve compartment, *Jk1* frequency did not differ between HDs, immunotherapy-naïve, and alemtuzumab-treated RRMS patients (**Supplementary Fig. 4A**). Further, naïve B cell usage of upstream *Vk* and downstream *Jk3,4,5* gene segments did not consistently separate subject groups (**Supplementary Fig. 4B**).

Discussion

We examined B cell tolerance mechanisms in the setting of RRMS and in vivo perturbation by alemtuzumab; the effect of transient CD52+ immune cell depletion on tolerance checkpoints had not been researched before. In addition, we combined an approach used historically for analysis of B cell checkpoint function involving construction of recombinant mAbs from post-checkpoint B cells with repertoire analysis by NGS. Again, this combination had not been applied —to our knowledge— beforehand.

The examination of central B cell tolerance checkpoints in individuals with autoimmune diseases indicates that these tolerance mechanisms are compromised, except in the case of MS, where they are heterogeneously distributed[13]. Although we did not directly examine polyreactivity of new emigrant B cells, which defines the

central checkpoint function, we examined polyreactivity of mature naïve B cells. This subset of mature naïve B cells comprise the next differentiation step for B cells after new emigrant B cells. As most polyrective B cells are removed before the new emigrant stage, with the polyreactive fraction remaining low thereafter, polyreactivity of mature naïve B cells could reflect central checkpoint integrity[26]. As we found no differences in mature naive polyreactivity between HDs, immunotherapy-naïve and alemtuzumab-treated RRMS patients, one could deduce that central checkpoint function is preserved in all subject groups. In accordance, we observed no differences in the frequency of IGKJ1, as well as upstream Vκ and downstream Jκ3□4□5 gene usage among subject groups in the NGS repertoire analysis, suggesting a similar extent of secondary recombination. Of note, secondary recombination and receptor editing constitute a main mechanism of central B cell tolerance [45,48–50]. These collective data are in agreement with previous research indicating that central tolerance checkpoint function is preserved in most MS patients[16] as opposed to rheumatoid arthritis (RA) [40,44].

After performing autoreactivity ELISA with mature naïve-derived mAbs, we found the peripheral B cell tolerance checkpoint likely compromised in two out of three immunotherapy-naïve and three out of six alemtuzumab-treated RRMS patients. Of note, previous investigations had found the peripheral checkpoint compromised in untreated relapsing MS patients (N=7)[16]. It should also be noted however that previously generated data showed that the autoreactive fraction can nearly overlap (approaching 30%) in some RRMS patients and HDs[13]. With these considerations taken into account, one can conclude that our results are not contrasting previous investigations. In alemtuzumab-treated patients, remarkably three out of six patients

showed preserved peripheral tolerance checkpoint function and very low autoreactive fractions, lower than those of HDs (p for the post-hoc comparison <0.05). This effect did not have clinical correlates and appeared to be stochastic however is likely attributable to CD52+ immune cell depletion with alemtuzumab. In some contrast (and a different setting), T1D patients treated with the anti-CD20 mAb rituximab did not regain function of the defective peripheral B cell tolerance checkpoint[17]. The differential action of rituximab and alemtuzumab could be explained by deeper depletion of B cells by alemtuzumab but also—and perhaps more so—by effective depletion of T cells including Tregs, known to influence peripheral checkpoint function[13,51]. Specifically, defective Tregs have been connected to defective peripheral B cell tolerance checkpoint function in both MS and IPEX, an inherited condition with FOXP3 deficiency [13,51–53]. In further support, Treg function is restored[54,55] post alemtuzumab application.

We additionally investigated whether defects in peripheral tolerance can directly lead to secondary autoimmunity, which often targets the thyroid in the form of Graves' disease and anti-TSHR antibodies [20]. We therefore tested mature naïve-derived mAbs against TSHR by CBA, however none of the tested mAbs showed binding with TSHR. Although we did not find evidence that TSHR autoantibody generation is a pre-germinal center event, this cannot be excluded since we tested relatively few cells/mAbs and autoantigen-specific B cells are rare.

The IgH CDR3 region plays a critical role in determining specificity toward antigens as well as repertoire diversity. Therefore, its composition and distinct physicochemical properties are of interest in the study of autoimmunity and may

correlate with B cell tolerance defects [15,24,56,57]. Previous studies examining autoimmune B cell repertoires have shown that IgH CDR3 regions of patients are longer[26,58], more hydrophobic[59], and more positively charged[60] compared to controls; moreover immunotherapy can influence CDR3 acidity[61]. Here, we found that in the naïve compartment of alemtuzumab-treated RRMS patients CDR3 net charge is significantly lower than in HDs, an effect that can be attributed to RRMS, alemtuzumab treatment, or both. The p value was just below 0.05—therefore not resistant to multiple comparison corrections—, constituting this finding exploratory. Indeed, future studies with larger study cohorts will very possibly render some of the identified differences significant or more significant. For example, we identified the known difference[34] between memory and naïve CDR3 length in HDs (decreased length in of memory compartment CDR3s), however this was not significant very likely due to the low N. Of interest and potential biological significance was the fact that while CDR3s were of shorter length in HD memory (primarily IgM) vs. naïve cells, they tended to be longer in the RRMS vs. HD naïve compartment (**Supplementary Fig. 2** and **Fig. 3**, respectively). As IgM memory B cells and plasma cells tend to be less poly- and autoreactive[47,62] (perhaps as a result of affinity maturation and selection pressure), longer naïve CDR3s in RRMS may represent a more sensitive marker of promiscuity/polyreactivity compared to examination of mature naïve-derived mAbs. Indeed, such antibody/B cell promiscuity has been reported previously[63–66] in RRMS mAbs, serum and CSF.

As memory cells likely play a critical role in MS immunology[67], we also examined whether memory IgH CDR3 properties differ between HDs and immunotherapy-naïve or alemtuzumab-treated RRMS patients. Indeed, we found significant differences in

IgD CDR3 length, polarity, and aromatic abundance between alemtuzumab-treated RRMS patients and HDs. Specifically, both RRMS and more so alemtuzumab treatment was associated with longer CDR3s. Interestingly, a similar effect was observed in RA patients treated with rituximab, where treatment was associated with longer IgD memory CDR3s and a lower IgD memory mutation acquisition rate[68]. Therefore, the increase in CDR3 length might have different contributors in RRMS and in alemtuzumab-treated RRMS. In the latter case -as in the case of rituximab in RA-, it likely is the transient B cell depletion by alemtuzumab or rituximab that leads to a repopulation similar to ontogeny, known to be associated with longer CDR3s[69].

Conclusion

We conducted a study whose main strength is the simultaneous, in-depth analysis of B cell reactivity and BCR repertoire diversity. This simultaneous measurement in the same subjects allowed for examination of correlation of the two parameters examined. Moreover, our study of disease and treatment mechanisms was performed with human samples and did not rely on animal models. Weaknesses include lack of longitudinal pre- and post-treatment samples, as alemtuzumab's application in our center was stopped due to a less favorable risk/benefit ratio compared to other treatments of RRMS such as B cell depletion. We compensated this lack with thorough matching cases with controls in regard to disease activity, sample acquisition time point, sex,

and age. Finally, our BCR NGS experiments are of an exploratory nature and comparisons would be strengthened with the addition of more subjects.

Our investigations show for the first time that transient CD52+ immune cell depletion could beneficially influence peripheral B cell tolerance checkpoint function in some patients, possibly through its action on Tregs. This mechanistic line of evidence may contribute to the explanation of alemtuzumab efficacy in RRMS. Secondary autoimmunity targeting the thyroid did not correlate with any of the measured B cell parameters and likely is a post-germinal center effect as conspicuous memory B cell expansions co-appear with autoimmune events[70]. Overall, our results illuminate both RRMS immunopathology as well as its *in vivo* perturbation by transient CD52+ immune cell depletion with alemtuzumab. Partial beneficial effects of alemtuzumab on B cell tolerance checkpoint function provide mechanistic support for potentially combining CD20+ with CD52+ immune cell depletion and reconstitution[71].

Data availability

Data will be shared upon reasonable personal request to the corresponding author.

Acknowledgments

The authors thank NEB for providing a Next® Immune Sequencing Kit, Chen Song of NEB for her valuable assistance with next generation sequencing quality control, Drs. Steven Kleinstein and Gisela Gabernet of Yale University for valuable discussions, and Dr. Sofia Grammenoudi from the BSRC Fleming cell sorting core facility for her support.

Funding

The study was funded by the Onassis Foundation.

Competing Interests

Anastasia Alexaki, Fotis Baltoumas, Georgios Pavlopoulos and Panos Stathopoulos have received research support by the Onassis Foundation. Dimitrios Tzanetakos, Panos Stathopoulos, Leonidas Stefanis, and Konstantinos Kilidireas participated in the phase IV trial of LEMTRADA® (alemtuzumab) treatment in patients with relapsing forms of MS (GZ402673-OBS13434). Chrysoula Zografou, Panos Stathopoulos, and Kevin O'Connor are founders of MABY. Galini Kyriakaki, Aglaia G. Vakrakou, Maria Anagnostouli, Georgia Karadima, Marinos C. Dalakas: nothing to disclose.

References

1. Leray E, Moreau T, Fromont A, Edan G. Epidemiology of multiple sclerosis. Rev Neurol (Paris). 2016;172(1):3-13. doi:10.1016/j.neurol.2015.10.006

2. Virgilio E, Vecchio D, Sarnelli MF, Solara V, Cantello R, Comi C. Early Predictors of Disability and Cognition in Multiple Sclerosis Patients: A Long-Term Retrospective Analysis. J Clin Med. 2023;12(2):685. doi:10.3390/jcm12020685

3. Lublin FD, Häring DA, Ganjgahi H, et al. How patients with multiple sclerosis acquire disability. Brain. 2022;145(9):3147-3161. doi:10.1093/brain/awac016

4. Alfredsson L, Olsson T. Lifestyle and Environmental Factors in Multiple Sclerosis. Cold Spring Harb Perspect Med. 2019;9(4):a028944. doi:10.1101/cshperspect.a028944

5. International Multiple Sclerosis Genetics Consortium. Multiple sclerosis genomic map implicates peripheral immune cells and microglia in susceptibility. Science. 2019;365(6460):eaav7188. doi:10.1126/science.aav7188

6. Pitt D, Lo CH, Gauthier SA, et al. Toward Precision Phenotyping of Multiple Sclerosis. Neurol Neuroimmunol Neuroinflamm. 2022;9(6):e200025. doi:10.1212/NXI.0000000000200025

7. Lassmann H, Brück W, Lucchinetti CF. The immunopathology of multiple sclerosis: an overview. Brain Pathol. 2007;17(2):210-218. doi:10.1111/j.1750-3639.2007.00064.x

8. Stadelmann C. Multiple sclerosis as a neurodegenerative disease: pathology, mechanisms and therapeutic implications. Curr Opin Neurol. 2011;24(3):224-229. doi:10.1097/WCO.0b013e328346056f

9. Lublin FD, Reingold SC, Cohen JA, et al. Defining the clinical course of multiple sclerosis. Neurology. 2014;83(3):278-286. doi:10.1212/WNL.0000000000000560

10. Gold R, Linington C, Lassmann H. Understanding pathogenesis and therapy of multiple sclerosis via animal models: 70 years of merits and culprits in experimental autoimmune encephalomyelitis research. Brain. 2006;129(8):1953-1971. doi:10.1093/brain/awl075

11. Cao Y, Goods BA, Raddassi K, et al. Functional inflammatory profiles distinguish myelin-reactive T cells from patients with multiple sclerosis. Sci Transl Med. 2015;7(287):287ra74. doi:10.1126/scitranslmed.aaa8038

12. Hauser SL, Bar-Or A, Comi G, et al. Ocrelizumab versus Interferon Beta-1a in Relapsing Multiple Sclerosis. N Engl J Med. 2017;376(3):221-234. doi:10.1056/NEJMoa1601277

13. Meffre E, O'Connor KC. Impaired B-cell tolerance checkpoints promote the development of autoimmune diseases and pathogenic autoantibodies. Immunol Rev. 2019;292(1):90-101. doi:10.1111/imr.12821

14. Cotzomi E, Stathopoulos P, Lee CS, et al. Early B cell tolerance defects in neuromyelitis optica favour anti-AQP4 autoantibody production. Brain. 2019;142(6):1598-1615. doi:10.1093/brain/awz106

15. Lee JY, Stathopoulos P, Gupta S, et al. Compromised fidelity of B-cell tolerance checkpoints in AChR and MuSK myasthenia gravis. Ann Clin Transl Neurol. 2016;3(6):443-454. doi:10.1002/acn3.311

16. Kinnunen T, Chamberlain N, Morbach H, et al. Specific peripheral B cell tolerance defects in patients with multiple sclerosis. J Clin Invest. 2013;123(6):2737-2741. doi:10.1172/JCI68775

17. Chamberlain N, Massad C, Oe T, Cantaert T, Herold KC, Meffre E. Rituximab does not reset defective early B cell tolerance checkpoints. J Clin Invest. 2016;126(1):282-287. doi:10.1172/JCI83840

18. Lünemann JD, Ruck T, Muraro PA, Bar-Or A, Wiendl H. Immune reconstitution therapies: concepts for durable remission in multiple sclerosis. Nat Rev Neurol. 2020;16(1):56-62. doi:10.1038/s41582-019-0268-z

19. Coles AJ, Twyman CL, Arnold DL, et al. Alemtuzumab for patients with relapsing multiple sclerosis after disease-modifying therapy: a randomised controlled phase 3 trial. Lancet. 2012;380(9856):1829-1839. doi:10.1016/S0140-6736(12)61768-1

20. Kazakou P, Tzanetakos D, Vakrakou AG, et al. Thyroid autoimmunity following alemtuzumab treatment in multiple sclerosis patients: a prospective study. Clin Exp Med. Published online January 15, 2023. doi:10.1007/s10238-022-00981-3

21. Rodig SJ, Abramson JS, Pinkus GS, et al. Heterogeneous CD52 expression among hematologic neoplasms: implications for the use of alemtuzumab (CAMPATH-1H). Clin Cancer Res. 2006;12(23):7174-7179. doi:10.1158/1078-0432.CCR-06-1275

22. Baker D, Herrod SS, Alvarez-Gonzalez C, Giovannoni G, Schmierer K. Interpreting Lymphocyte Reconstitution Data From the Pivotal Phase 3 Trials of Alemtuzumab. JAMA Neurology. 2017;74(8):961-969. doi:10.1001/jamaneurol.2017.0676

23. Zhang X, Tao Y, Chopra M, et al. Differential reconstitution of T cell subsets following immunodepleting treatment with alemtuzumab (anti-CD52 monoclonal antibody) in patients with relapsing-remitting multiple sclerosis. J Immunol. 2013;191(12):5867-5874. doi:10.4049/jimmunol.1301926

24. Vander Heiden JA, Stathopoulos P, Zhou JQ, et al. Dysregulation of B Cell Repertoire Formation in Myasthenia Gravis Patients Revealed through Deep Sequencing. J Immunol. 2017;198(4):1460-1473. doi:10.4049/jimmunol.1601415

25. Thompson AJ, Banwell BL, Barkhof F, et al. Diagnosis of multiple sclerosis: 2017 revisions of the McDonald criteria. The Lancet Neurology. 2018;17(2):162-173. doi:10.1016/S1474-4422(17)30470-2

26. Wardemann H, Yurasov S, Schaefer A, Young JW, Meffre E, Nussenzweig MC. Predominant autoantibody production by early human B cell precursors. Science. 2003;301(5638):1374-1377. doi:10.1126/science.1086907

27. Menard L, Samuels J, Ng YS, Meffre E. Inflammation-independent defective early B cell tolerance checkpoints in rheumatoid arthritis. Arthritis Rheum. 2011;63(5):1237-1245. doi:10.1002/art.30164

28. Ye J, Ma N, Madden TL, Ostell JM. IgBLAST: an immunoglobulin variable domain sequence analysis tool. Nucleic Acids Res. 2013;41(Web Server issue):W34-40. doi:10.1093/nar/gkt382

29. Brochet X, Lefranc MP, Giudicelli V. IMGT/V-QUEST: the highly customized and integrated system for IG and TR standardized V-J and V-D-J sequence analysis. Nucleic Acids Res. 2008;36(Web Server issue):W503-508. doi:10.1093/nar/gkn316

30. Takata K, Stathopoulos P, Cao M, et al. Characterization of pathogenic monoclonal autoantibodies derived from muscle-specific kinase myasthenia gravis patients. JCI Insight. 2019;4(12):e127167, 127167. doi:10.1172/jci.insight.127167

31. Stathopoulos P, Chastre A, Waters P, et al. Autoantibodies against Neurologic Antigens in Nonneurologic Autoimmunity. J Immunol. 2019;202(8):2210-2219. doi:10.4049/jimmunol.1801295

32. Jiang R, Fichtner ML, Hoehn KB, et al. Single-cell repertoire tracing identifies rituximab-resistant B cells during myasthenia gravis relapses. JCI Insight. 2020;5(14):e136471, 136471. doi:10.1172/jci.insight.136471

33. Vander Heiden JA, Yaari G, Uduman M, et al. pRESTO: a toolkit for processing high-throughput sequencing raw reads of lymphocyte receptor repertoires. Bioinformatics. 2014;30(13):1930-1932. doi:10.1093/bioinformatics/btu138

34. Wu YC, Kipling D, Leong HS, Martin V, Ademokun AA, Dunn-Walters DK. High-throughput immunoglobulin repertoire analysis distinguishes between human IgM memory and switched memory B-cell populations. Blood. 2010;116(7):1070-1078. doi:10.1182/blood-2010-03-275859

35. Lanzolla G, Marinò M, Menconi F. Graves disease: latest understanding of pathogenesis and treatment options. Nat Rev Endocrinol. 2024;20(11):647-660. doi:10.1038/s41574-024-01016-5

36. Sanders J, Evans M, Premawardhana LDKE, et al. Human monoclonal thyroid stimulating autoantibody. Lancet. 2003;362(9378):126-128. doi:10.1016/s0140-6736(03)13866-4

37. Morbach H, Eichhorn EM, Liese JG, Girschick HJ. Reference values for B cell subpopulations from infancy to adulthood. Clin Exp Immunol. 2010;162(2):271-279. doi:10.1111/j.1365-2249.2010.04206.x

38. Shiokawa S, Mortari F, Lima JO, et al. IgM heavy chain complementarity-determining region 3 diversity is constrained by genetic and somatic mechanisms until two months after birth. J Immunol. 1999;162(10):6060-6070.

39. Bridges SL, Lee SK, Johnson ML, et al. Somatic mutation and CDR3 lengths of immunoglobulin kappa light chains expressed in patients with rheumatoid arthritis and in normal individuals. J Clin Invest. 1995;96(2):831-841. doi:10.1172/JCI118129

40. Samuels J, Ng YS, Coupillaud C, Paget D, Meffre E. Impaired early B cell tolerance in patients with rheumatoid arthritis. J Exp Med. 2005;201(10):1659-1667. doi:10.1084/jem.20042321

41. Steinel NC, Lee BS, Tubbs AT, et al. The ataxia telangiectasia mutated kinase controls Igκ allelic exclusion by inhibiting secondary Vκ-to-Jκ rearrangements. J Exp Med. 2013;210(2):233-239. doi:10.1084/jem.20121605

42. Rajewsky K. Clonal selection and learning in the antibody system. Nature. 1996;381(6585):751-758. doi:10.1038/381751a0

43. Nemazee D. Receptor editing in lymphocyte development and central tolerance. Nat Rev Immunol. 2006;6(10):728-740. doi:10.1038/nri1939

44. Mensah KA, Chen JW, Schickel JN, et al. Impaired ATM activation in B cells is associated with bone resorption in rheumatoid arthritis. Sci Transl Med. 2019;11(519):eaaw4626. doi:10.1126/scitranslmed.aaw4626

45. Nemazee D. Mechanisms of central tolerance for B cells. Nat Rev Immunol. 2017;17(5):281-294. doi:10.1038/nri.2017.19

46. Tiller T, Tsuiji M, Yurasov S, Velinzon K, Nussenzweig MC, Wardemann H. Autoreactivity in Human IgG+ Memory B Cells. Immunity. 2007;26(2):205-213. doi:10.1016/j.immuni.2007.01.009

47. Tsuiji M, Yurasov S, Velinzon K, Thomas S, Nussenzweig MC, Wardemann H. A checkpoint for autoreactivity in human IgM+ memory B cell development. J Exp Med. 2006;203(2):393-400. doi:10.1084/jem.20052033

48. Luning Prak ET, Monestier M, Eisenberg RA. B cell receptor editing in tolerance and autoimmunity. Ann N Y Acad Sci. 2011;1217:96-121. doi:10.1111/j.1749-6632.2010.05877.x

49. Gauld SB, Merrell KT, Cambier JC. Silencing of autoreactive B cells by anergy: a fresh perspective. Curr Opin Immunol. 2006;18(3):292-297. doi:10.1016/j.coi.2006.03.015

50. Halverson R, Torres RM, Pelanda R. Receptor editing is the main mechanism of B cell tolerance toward membrane antigens. Nat Immunol. 2004;5(6):645-650. doi:10.1038/ni1076

51. Kinnunen T, Chamberlain N, Morbach H, et al. Accumulation of peripheral autoreactive B cells in the absence of functional human regulatory T cells. Blood. 2013;121(9):1595-1603. doi:10.1182/blood-2012-09-457465

52. Janssen E, Morbach H, Ullas S, et al. Dedicator of cytokinesis 8-deficient patients have a breakdown in peripheral B-cell tolerance and defective regulatory T cells. J Allergy Clin Immunol. 2014;134(6):1365-1374. doi:10.1016/j.jaci.2014.07.042

53. Sng J, Ayoglu B, Chen JW, et al. AIRE expression controls the peripheral selection of autoreactive B cells. Sci Immunol. 2019;4(34):eaav6778. doi:10.1126/sciimmunol.aav6778

54. Dominguez-Villar M, Baecher-Allan CM, Hafler DA. Identification of T helper type 1–like, Foxp3+ regulatory T cells in human autoimmune disease. Nat Med. 2011;17(6):673-675. doi:10.1038/nm.2389

55. Haas J, Würthwein C, Korporal-Kuhnke M, et al. Alemtuzumab in Multiple Sclerosis: Short- and Long-Term Effects of Immunodepletion on the Peripheral Treg Compartment. Front Immunol. 2019;10. doi:10.3389/fimmu.2019.01204

56. Xu JL, Davis MM. Diversity in the CDR3 region of V(H) is sufficient for most antibody specificities. Immunity. 2000;13(1):37-45. doi:10.1016/s1074-7613(00)00006-6

57. Stathopoulos P, Kumar A, Heiden JAV, Pascual-Goñi E, Nowak RJ, O'Connor KC. Mechanisms underlying B cell immune dysregulation and autoantibody production in MuSK myasthenia gravis. Ann N Y Acad Sci. 2018;1412(1):154-165. doi:10.1111/nyas.13535

58. Larimore K, McCormick MW, Robins HS, Greenberg PD. Shaping of human germline IgH repertoires revealed by deep sequencing. J Immunol. 2012;189(6):3221-3230. doi:10.4049/jimmunol.1201303

59. Meffre E, Schaefer A, Wardemann H, Wilson P, Davis E, Nussenzweig MC. Surrogate light chain expressing human peripheral B cells produce self-reactive antibodies. J Exp Med. 2004;199(1):145-150. doi:10.1084/jem.20031550

60. Richardson C, Chida AS, Adlowitz D, et al. Molecular Basis of 9G4 B Cell Autoreactivity in Human Systemic Lupus Erythematosus. J Immunol. 2013;191(10):4926-4939. doi:10.4049/jimmunol.1202263

61. Huang W, Quach TD, Dascalu C, et al. Belimumab promotes negative selection of activated autoreactive B cells in systemic lupus erythematosus patients. JCI Insight. 2018;3(17):e122525, 122525. doi:10.1172/jci.insight.122525

62. Scheid JF, Mouquet H, Kofer J, Yurasov S, Nussenzweig MC, Wardemann H. Differential regulation of self-reactivity discriminates between IgG+ human circulating memory B cells and bone marrow plasma cells. Proc Natl Acad Sci U S A. 2011;108(44):18044-18048. doi:10.1073/pnas.1113395108

63. Quintana FJ, Farez MF, Viglietta V, et al. Antigen microarrays identify unique serum autoantibody signatures in clinical and pathologic subtypes of multiple sclerosis. Proceedings of the National Academy of Sciences. 2008;105(48):18889-18894. doi:10.1073/pnas.0806310105

64. Brändle SM, Obermeier B, Senel M, et al. Distinct oligoclonal band antibodies in multiple sclerosis recognize ubiquitous self-proteins. Proc Natl Acad Sci U S A. 2016;113(28):7864-7869. doi:10.1073/pnas.1522730113

65. Willis SN, Stathopoulos P, Chastre A, Compton SD, Hafler DA, O'Connor KC. Investigating the Antigen Specificity of Multiple Sclerosis Central Nervous System-Derived Immunoglobulins. Front Immunol. 2015;6:600. doi:10.3389/fimmu.2015.00600

66. Quintana FJ, Farez MF, Izquierdo G, Lucas M, Cohen IR, Weiner HL. Antigen microarrays identify CNS-produced autoantibodies in RRMS. Neurology. 2012;78(8):532-539. doi:10.1212/WNL.0b013e318247f9f3

67. Jelcic I, Nimer FA, Wang J, et al. Memory B Cells Activate Brain-Homing, Autoreactive CD4+ T Cells in Multiple Sclerosis. Cell. 2018;175(1):85-100.e23. doi:10.1016/j.cell.2018.08.011

68. Muhammad K, Roll P, Einsele H, Dörner T, Tony HP. Delayed acquisition of somatic hypermutations in repopulated IGD+CD27+ memory B cell receptors after rituximab treatment. Arthritis Rheum. 2009;60(8):2284-2293. doi:10.1002/art.24722

69. Souto-Carneiro MM, Sims GP, Girschik H, Lee J, Lipsky PE. Developmental changes in the human heavy chain CDR3. J Immunol. 2005;175(11):7425-7436. doi:10.4049/jimmunol.175.11.7425

70. Ruck T, Barman S, Schulte-Mecklenbeck A, et al. Alemtuzumab-induced immune phenotype and repertoire changes: implications for secondary autoimmunity. Brain. 2022;145(5):1711-1725. doi:10.1093/brain/awac064

71. Meltzer E, Campbell S, Ehrenfeld B, et al. Mitigating alemtuzumab-associated autoimmunity in MS: A “whack-a-mole” B-cell depletion strategy. Neurol Neuroimmunol Neuroinflamm. 2020;7(6):e868. doi:10.1212/NXI.0000000000000868

Table

Samples	Age range[1]	Sex	Time to sampling[2]	MS activity	Secondary autoimmunity	Tolerance assay	Defective peripheral checkpoint	BCR NGS
HD01[3]	26-30	F	NA	NA	NA	Yes	No	No
HD02[3]	46-50	M	NA	NA	NA	Yes	No	No
HD13	31-35	F	NA	NA	NA	No	NA	Yes
HD18	36-40	F	NA	NA	NA	Yes	No	Yes
HD19	41-45	M	NA	NA	NA	No	NA	Yes
RRMS09	46-50	F	NA	NA	NA	No	NA	Yes
RRMS16	41-45	F	NA	NA	NA	Yes	Yes	Yes
RRMS17	26-30	F	NA	NA	NA	Yes	Yes	Yes
RRMS21	26-30	M	NA	NA	NA	Yes	No	Yes
Ale27	36-40	F	3.9	No	No	Yes	No	Yes
Ale40	36-40	F	3.6	No	No	Yes	Yes	Yes
Ale46	31-35	F	2.2	No	No	Yes	No	No
Ale03	36-40	M	3.9	No	Yes (Graves)	Yes	Yes	Yes
Ale25	26-30	F	3.7	No	Yes (Graves)	Yes	No	Yes
Ale26	51-55	F	3.8	No	Yes (Hashimoto)	No	NA	Yes
Ale33	36-40	M	3.5	No	Yes (Hashimoto)	Yes	Yes	No
Ale24	41-45	M	3.5	Yes	Yes (ITP)	No	NA	Yes
Ale29	36-40	M	4.8	Yes	Yes (ITP)	No	NA	Yes

[1]Age range at the time of sample acquisition. [2]Time to sampling in years was defined as the interval between initial dose of alemtuzumab and collection of the sample. [3]Studied by the laboratory of KC O'Connor at Yale University[15]. None of the subjects carried the PTPN22 R620W polymorphism. Ale: Alemtuzumab-treated RRMS patients; F: Female; HD: Healthy donor; ITP: Immune Thrombocytopenia; M: Male; NA: Not applicable; RRMS: Relapsing-remitting multiple sclerosis.

Table. Characteristics of study subjects

Figure legends

Figure 1. Mature naïve B cell polyreactivity is similar in healthy donors, immunotherapy-naïve RRMS patients, and alemtuzumab-treated RRMS patients. (**A)** Mature naïve B cell-derived mAbs from 3 HDs, 3 immunotherapy-naïve and 6 alemtuzumab-treated RRMS patients were tested for their reactivity against dsDNA, LPS, and insulin by ELISA. ODs are shown on the y axis and mAbs concentrations on the x axis. Solid lines connect OD values of each mAb at a given dilution, and each point represents the mean of biological duplicates. Dotted curves represent positive control mAb ED38 binding; horizontal dotted lines represent the positivity cutoff. Below, black-filled areas of pie charts indicate the frequency of polyreactive mAbs for each subject, while the number in the center of each pie chart indicates the number of cloned mAbs per subject. (**B)** Polyreactivity frequencies in HDs, immunotherapy-naïve and alemtuzumab-treated RRMS patents, with lines representing mean values. Means did not differ significantly. Ale: Alemtuzumab-treated RRMS patients; dsDNA: Double-stranded DNA; HD: Healthy donor; LPS: Lipopolysaccharide; mAb: monoclonal antibody; RRMS: Relapsing-remitting multiple sclerosis.

Figure 2. Alemtuzumab alters peripheral B cell tolerance checkpoint function in a fraction of RRMS patients. (**A)** Mature naïve B cell-derived mAbs from 3 HDs, 3 immunotherapy-naïve and 6 alemtuzumab-treated RRMS patients were tested for their reactivity against HEp-2 cell lysate. ODs are shown on the y axis and mAbs concentrations on the x axis. Solid lines connect OD values of each mAb at a given dilution, and each point represents the mean of biological duplicates. Dotted curves represent positive control mAb ED38 binding; horizontal dotted lines represent the

positivity cutoff. Below, black-filled areas of pie charts indicate the frequency of autoreactive mAbs for each subject, while the number in the center of each pie chart indicates the number of cloned mAbs per subject. **(B)** Autoreactivity frequencies in HDs, immunotherapy-naïve and alemtuzumab-treated RRMS patents, with lines representing mean values. Means did not differ significantly. Ale: Alemtuzumab-treated RRMS patients; HEp-2: Human Epithelial Type 2 cells; HD: Healthy donor; RRMS: Relapsing-remitting multiple sclerosis.

Figure 3. NGS analysis of naïve IgH CDR3 properties in HD, immunotherapy-naïve, and alemtuzumab-treated RRMS subjects. The following properties were calculated per Ig class: **(A)** CDR3 length, **(B)** the grand average hydropathy index (GRAVY), **(C)** net charge, **(D)** polarity, **(E)** side chain bulkiness, **(F)** aliphatic index, **(G)** aromatic abundance, **(H)** acidic abundance, and **(I)** basic abundance. Black circles represent individual HD values, black squares those of immunotherapy-naïve RRMS patients and triangles those of alemtuzumab-treated RRMS patients. Among the latter, green triangles represent alemtuzumab-treated patients without signs of MS activity and secondary autoimmunity, orange triangles alemtuzumab-treated patients with both signs of MS activity and of secondary autoimmunity, and black triangles alemtuzumab-treated patients without MS activity but with secondary autoimmunity. Differences between groups (HD, immunotherapy-naïve RRMS, and alemtuzumab-treated RRMS) were tested with the Mann-Whitney test, and p values are indicated when significant (**$P \leq 0.01$; *$P \leq 0.05$). ALE: Alemtuzumab-treated RRMS patients; CDR: Complementarity-Determining Region; HD: Healthy donor; Ig: immunoglobulin; IgH: heavy chain; NGS: Next-generation sequencing; RRMS: Relapsing-remitting multiple sclerosis.

Figure 4. The usage of *Jk1*, upstream *Vk*, and downstream *Jk3,4,5* gene segments of Igk in mature naive B cells do not differ among study groups. (A) Collective data on *Jk1* gene usage frequency across all study groups. **(B)** Upstream *Vk* gene usage frequency was plotted against downstream *Jk3,4,5* usage in mature naive B cells from all study specimens. Among the latter, green triangles represent alemtuzumab-treated patients without signs of MS activity and secondary autoimmunity, orange triangles alemtuzumab-treated patients with both signs of MS activity and of secondary autoimmunity, and black triangles alemtuzumab-treated patients without MS activity but with secondary autoimmunity. Differences between groups (HD, immunotherapy-naïve RRMS, and alemtuzumab-treated RRMS) were tested with the Mann-Whitney test, and p values are indicated when significant (**$P \leq 0.01$; *$P \leq 0.05$). ALE: Alemtuzumab-treated RRMS patients; HD: Healthy donor; RRMS: Relapsing-remitting multiple sclerosis.

Figure 5. NGS analysis of memory IgH CDR3 properties in HD, immunotherapy-naïve, and alemtuzumab-treated RRMS subjects. The following properties were calculated per Ig class: **(A)** CDR3 length, **(B)** the grand average hydropathy index (GRAVY), **(C)** net charge, **(D)** polarity, **(E)** side chain bulkiness, **(F)** aliphatic index, **(G)** aromatic abundance, **(H)** acidic abundance, and **(I)** basic abundance. Black circles represent individual HD values, black squares those of immunotherapy-naïve RRMS patients and triangles those of alemtuzumab-treated RRMS patients. Among the latter, green triangles represent alemtuzumab-treated patients without signs of MS activity and secondary autoimmunity, orange triangles alemtuzumab-treated patients with both signs of MS activity and of secondary

autoimmunity, and black triangles alemtuzumab-treated patients without MS activity but with secondary autoimmunity. Differences between groups (HD, immunotherapy-naïve RRMS, and alemtuzumab-treated RRMS) were tested with the Mann-Whitney test, and p values are indicated when significant (**$P \leq 0.01$; *$P \leq 0.05$). ALE: Alemtuzumab-treated RRMS patients; CDR: Complementarity-Determining Region; HD: Healthy donor; Ig: immunoglobulin; IgH: heavy chain; NGS: Next-generation sequencing; RRMS: Relapsing-remitting multiple sclerosis.

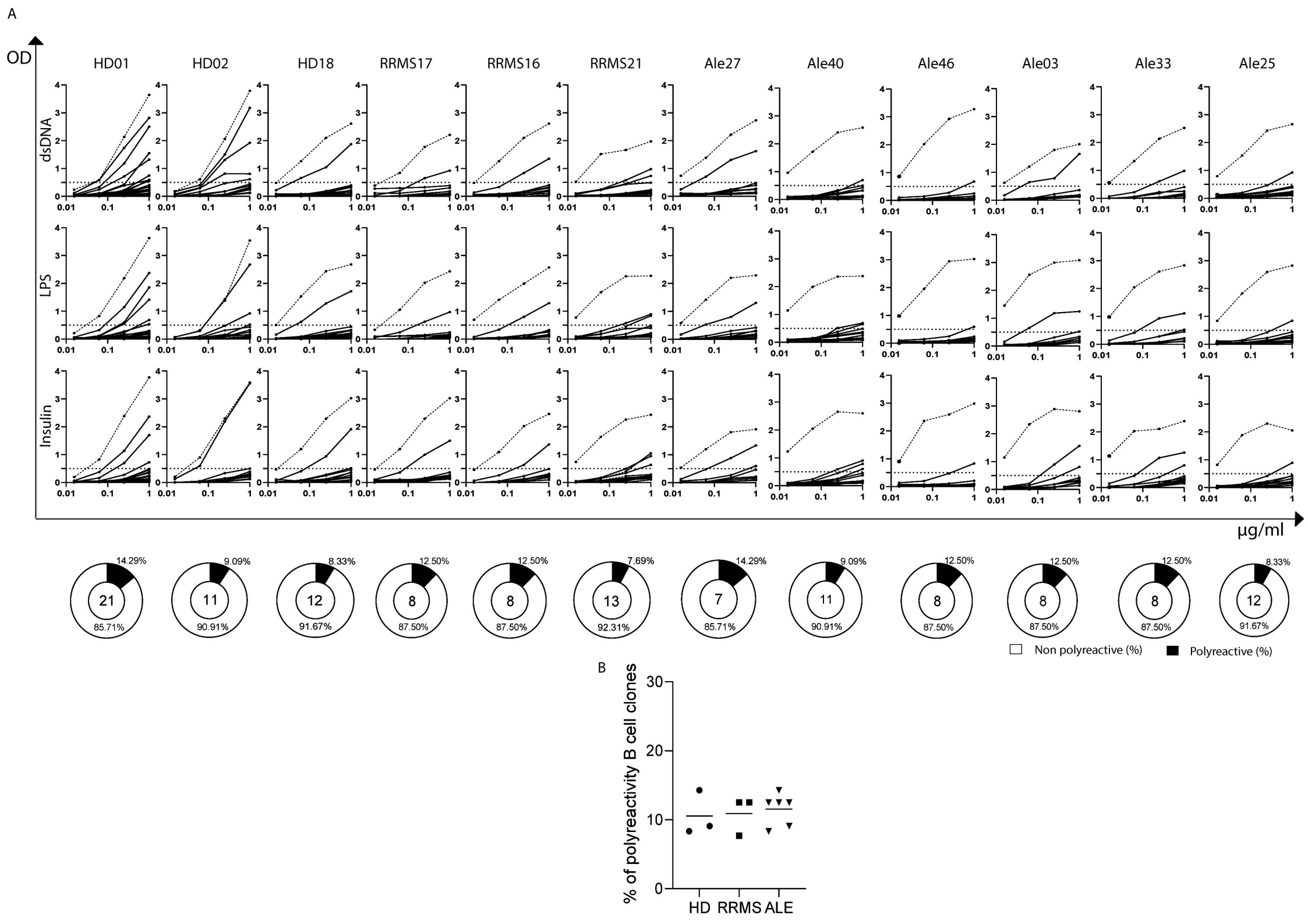
A
OD
HD01
HD02
HD18
RRMS17
RRMS16
RRMS21
Ale27
Ale40
Ale46
Ale03
Ale33
Ale25
dsDNA
LPS
Insulin
µg/ml
14.29%
21
85.71%
9.09%
11
90.91%
8.33%
12
91.67%
12.50%
8
87.50%
12.50%
8
87.50%
7.69%
13
92.31%
14.29%
7
85.71%
9.09%
11
90.91%
12.50%
8
87.50%
12.50%
8
87.50%
12.50%
8
87.50%
8.33%
12
91.67%
Non polyreactive (%)
Polyreactive (%)
B
% of polyreactivity B cell clones
HD
RRMS
ALE

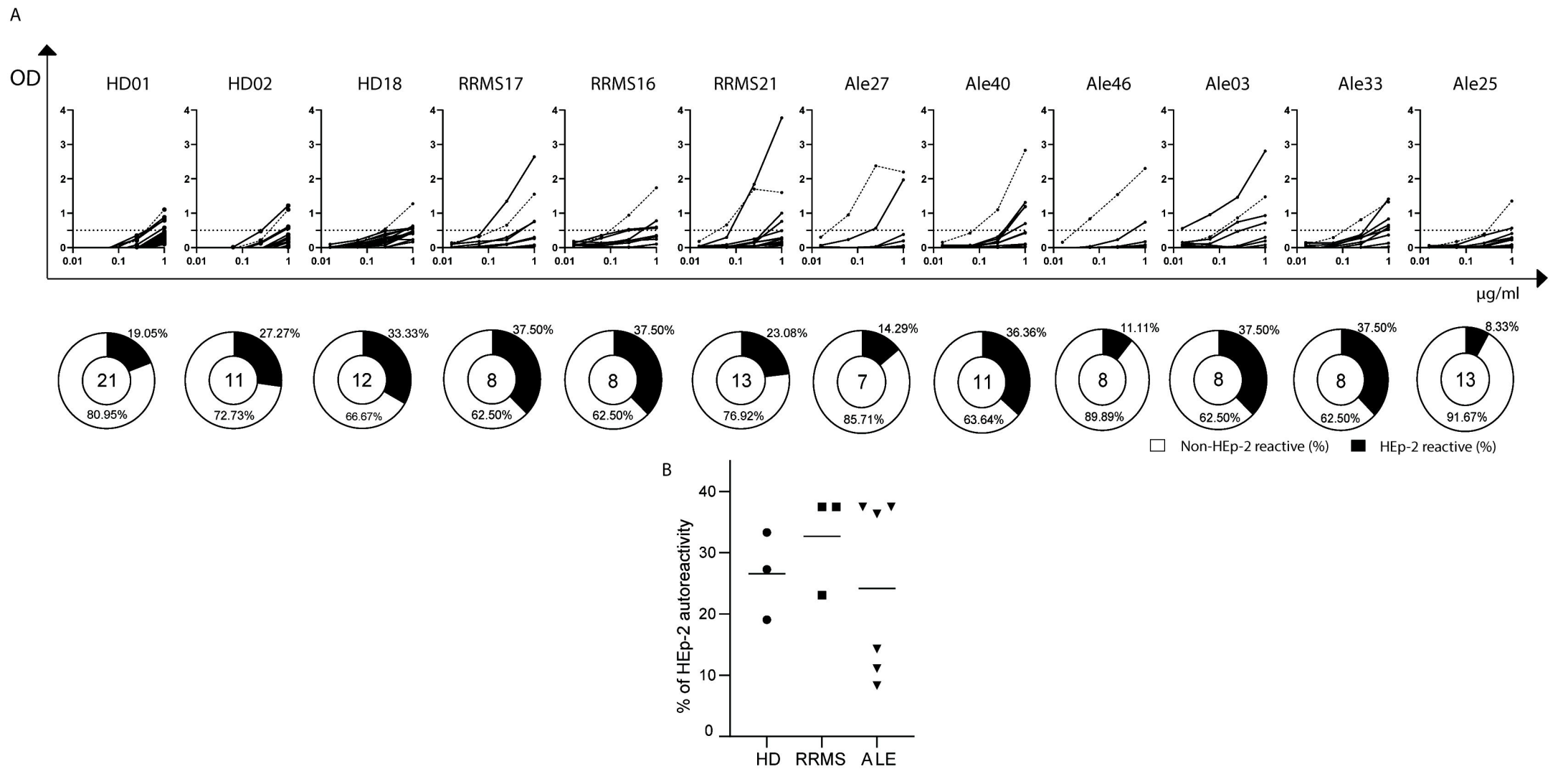
A
OD
HD01
HD02
HD18
RRMS17
RRMS16
RRMS21
Ale27
Ale40
Ale46
Ale03
Ale33
Ale25
0.01
0.1
1
µg/ml
19.05%
21
80.95%
27.27%
11
72.73%
33.33%
12
66.67%
37.50%
8
62.50%
37.50%
8
62.50%
23.08%
13
76.92%
14.29%
7
85.71%
36.36%
11
63.64%
11.11%
8
89.89%
37.50%
8
62.50%
37.50%
8
62.50%
8.33%
13
91.67%
Non-HEp-2 reactive (%)
HEp-2 reactive (%)
B
% of HEp-2 autoreactivity
HD
RRMS
ALE

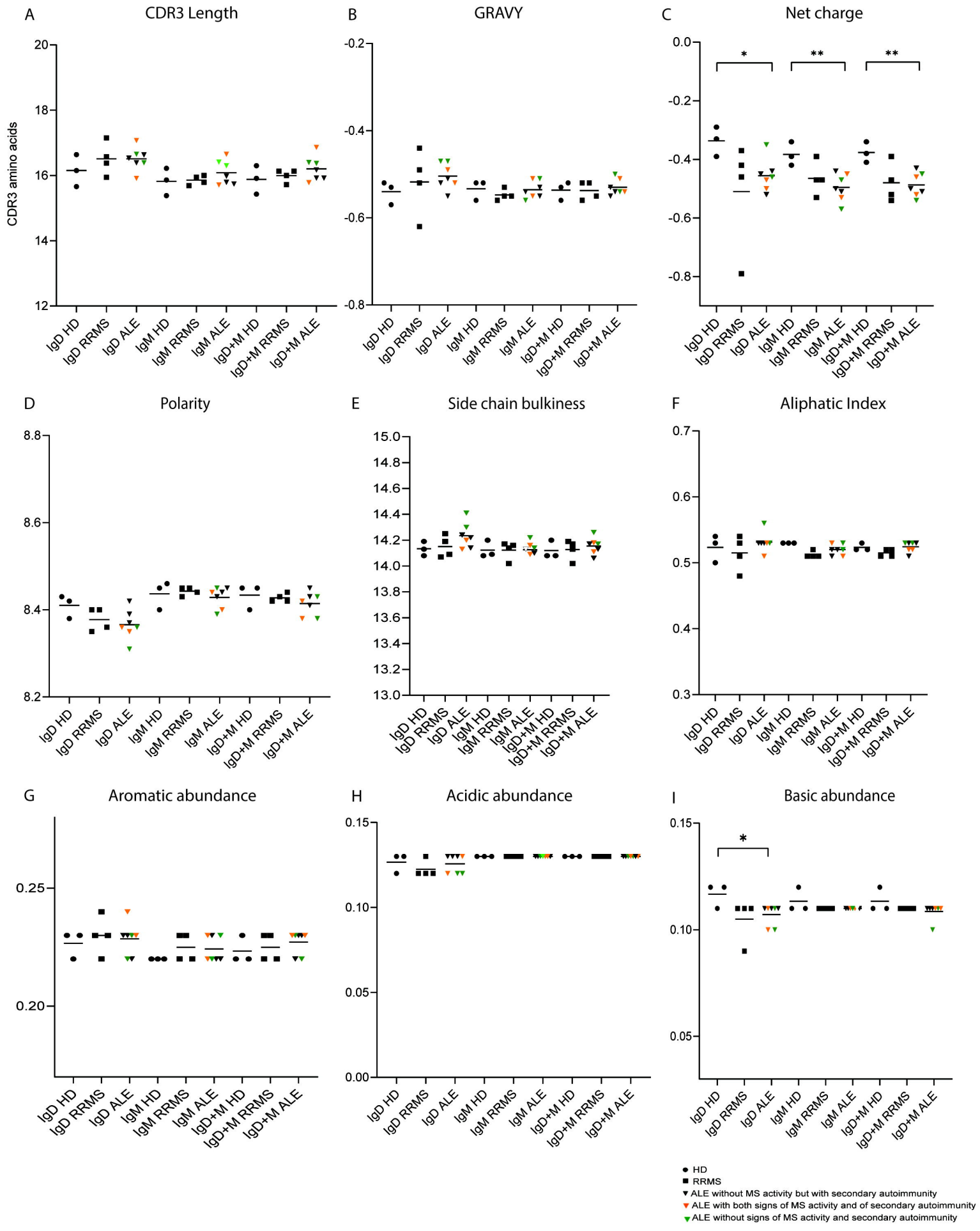
A
CDR3 Length
CDR3 amino acids
B
GRAVY
C
Net charge
D
Polarity
E
Side chain bulkiness
F
Aliphatic Index
G
Aromatic abundance
H
Acidic abundance
I
Basic abundance
IgD HD
IgD RRMS
IgD ALE
IgM HD
IgM RRMS
IgM ALE
IgD+M HD
IgD+M RRMS
IgD+M ALE
HD
RRMS
ALE without MS activity but with secondary autoimmunity
ALE with both signs of MS activity and of secondary autoimmunity
ALE without signs of MS activity and secondary autoimmunity

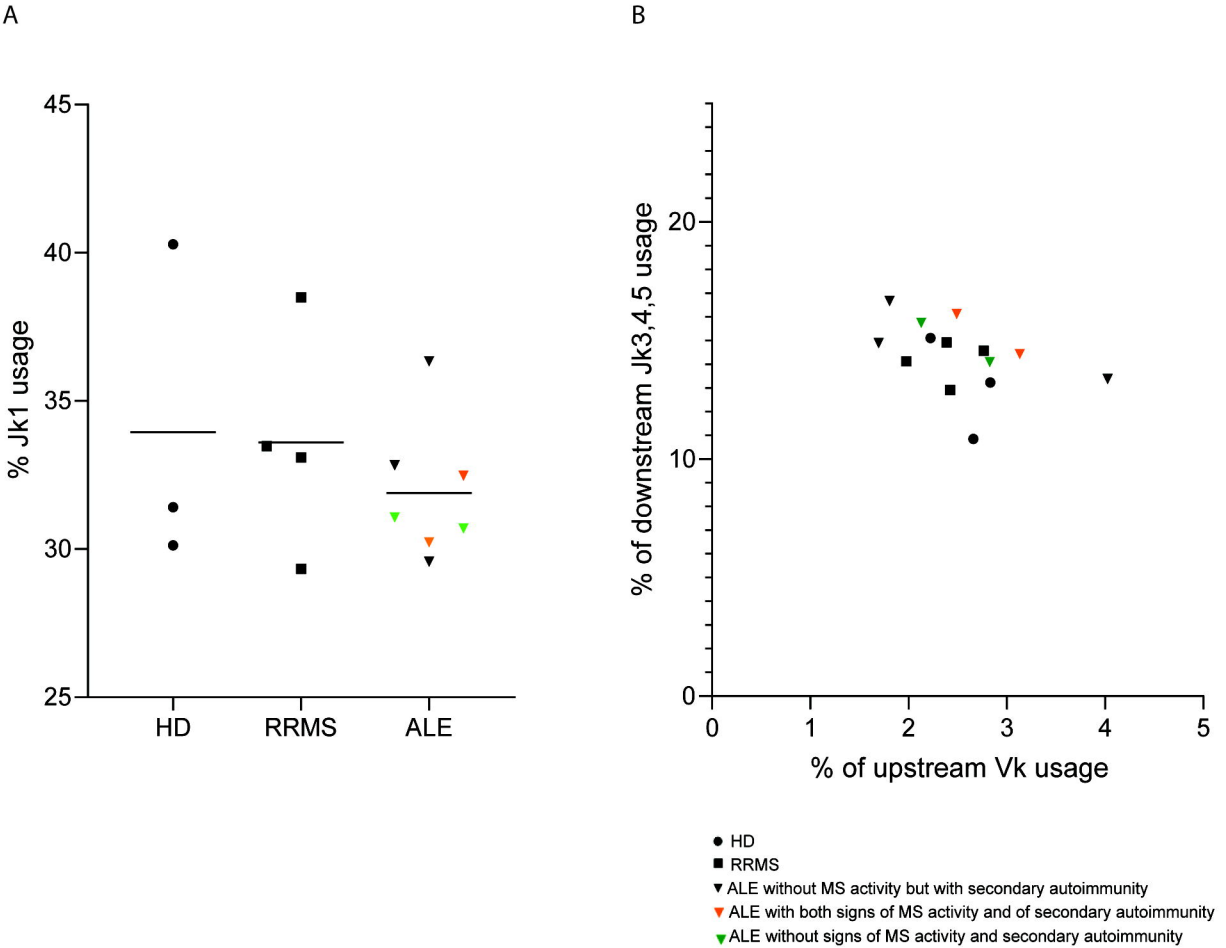
A
B
% Jk1 usage
45
40
35
30
25
HD
RRMS
ALE
% of downstream Jk3,4,5 usage
20
10
0
0
1
2
3
4
5
% of upstream Vk usage
HD
RRMS
ALE without MS activity but with secondary autoimmunity
ALE with both signs of MS activity and of secondary autoimmunity
ALE without signs of MS activity and secondary autoimmunity

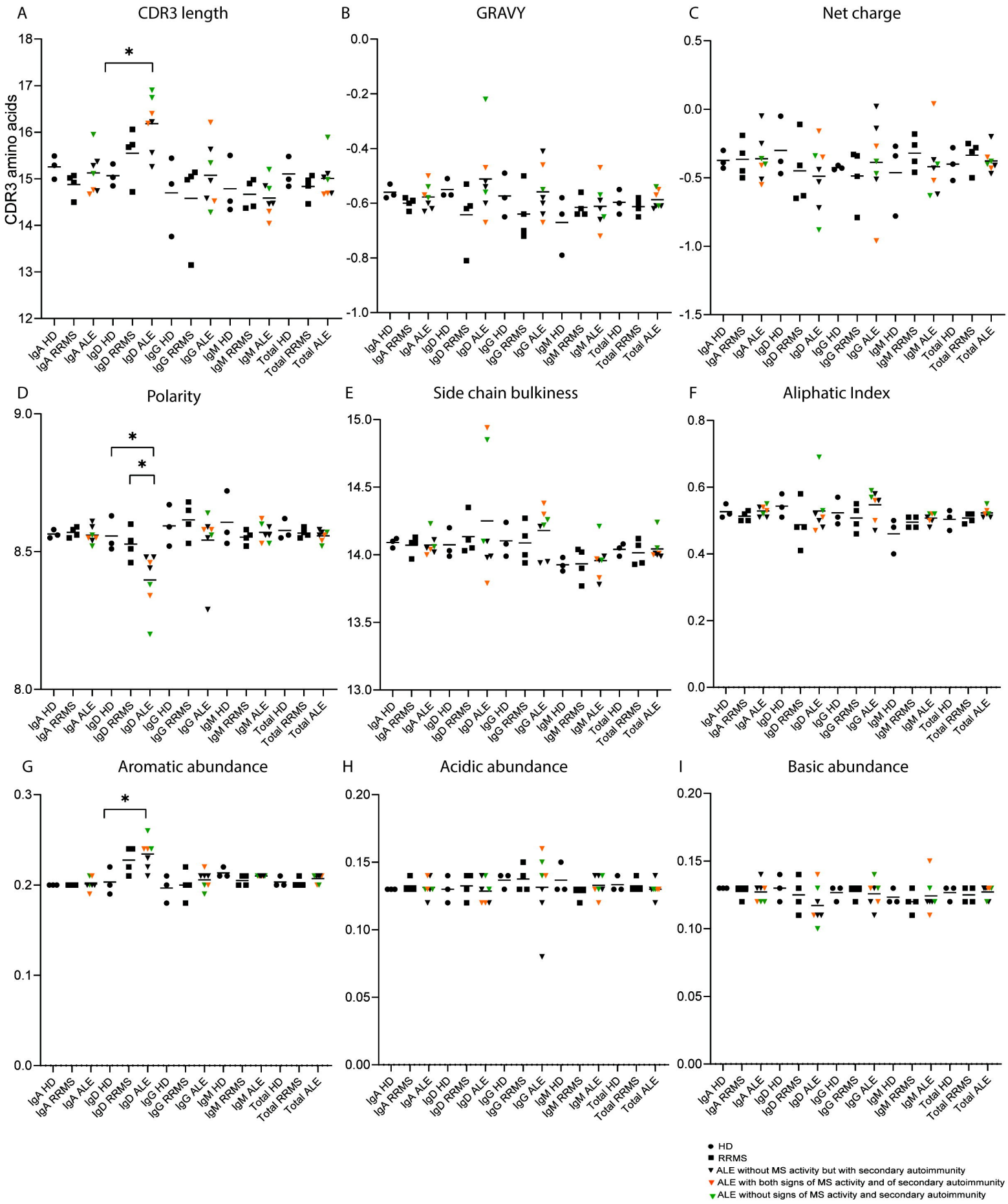
A
CDR3 length
CDR3 amino acids
B
GRAVY
C
Net charge
D
Polarity
E
Side chain bulkiness
F
Aliphatic Index
G
Aromatic abundance
H
Acidic abundance
I
Basic abundance
IgA HD
IgA RRMS
IgA ALE
IgD HD
IgD RRMS
IgD ALE
IgG HD
IgG RRMS
IgG ALE
IgM HD
IgM RRMS
IgM ALE
Total HD
Total RRMS
Total ALE
HD
RRMS
ALE without MS activity but with secondary autoimmunity
ALE with both signs of MS activity and of secondary autoimmunity
ALE without signs of MS activity and secondary autoimmunity